AGU100 ADVANCING EARTH AND SPACE SCIENCE

Geophysical Research Letters

RESEARCH LETTER
10.1029/2018GL078504

Key Points:
- CMIP5 models with good MJO simulations are used to examine the changes of MJO precipitation and wind variance under global warming
- Global warming enhances MJO precipitation amplitude while weakening the MJO circulation in most models and in the multimodel mean
- Future changes in the ratio of MJO precipitation to wind variance are mediated by the increase in the vertical dry static energy gradient in the tropics

Supporting Information:
- Supporting Information S1

Correspondence to:
H. X. Bui,
hien.bui@colostate.edu

Citation:
Bui, H. X., & Maloney, E. D. (2018). Changes in Madden-Julian oscillation precipitation and wind variance under global warming. *Geophysical Research Letters*, *45*, 7148–7155. https://doi.org/10.1029/2018GL078504

Received 24 APR 2018
Accepted 22 JUN 2018
Accepted article online 3 JUL 2018
Published online 16 JUL 2018

Changes in Madden-Julian Oscillation Precipitation and Wind Variance Under Global Warming

Hien X. Bui[1] **and Eric D. Maloney**[1]

[1]Department of Atmospheric Science, Colorado State University, Fort Collins, CO, USA

Abstract The Madden-Julian oscillation (MJO) is the leading mode of tropical intraseasonal variability, having profound impacts on many weather and climate phenomena across the tropics and extratropics. Previous studies using a limited number of models have suggested complex changes in MJO activity in a warmer climate. While most studies have argued that MJO precipitation amplitude will increase in a future warmer climate, others note that this is not necessarily the case for MJO wind variability. This distinction is important since MJO wind fluctuations are responsible for producing remote impacts on extreme weather through teleconnections. In this study, we examine projected changes of MJO precipitation and wind variance at the end of the 21st century in Representative Concentration Pathway 8.5 using the multimodel Coupled Model Intercomparison Project phase 5 data set. Under global warming, most models show an increase in MJO band precipitation variance, while wind variability decreases. The discrepancy between MJO precipitation and wind variance changes under global warming is shown to be due to increases in tropical static stability in a warmer climate. The multimodel mean shows a 20% increase in both the 500-hPa vertical tropical dry static energy gradient and the ratio of intraseasonal precipitation to 500 hPa omega fluctuations, consistent with scaling by weak temperature gradient theory. These results imply that tropical static stability increases may weaken the MJO's ability to influence extreme events in future warmer climate by weakening wind teleconnections, even though MJO precipitation amplitude may increase.

Plain Language Summary The Madden-Julian oscillation has profound impacts on weather and climate phenomena over the tropical and extratropical regions, including a modulation of atmospheric rivers, hurricanes, and atmospheric blocking. We can currently exploit knowledge of the MJO to predict such phenomena several weeks in advance. Therefore, understanding how the MJO may change under global warming is important to understanding its future impacts and for prediction. In this manuscript, we show how MJO precipitation and wind variance change at the end of the 21st Century under global warming (RCP8.5) using the CMIP5 multi-model dataset. We derive the interesting result that global warming enhances MJO precipitation amplitude while weakening the MJO circulation. This result is important, as MJO teleconnections to other parts of the world are mediated by the circulation response, and our results suggest that MJO impacts on atmospheric rivers, hurricanes, and other extreme events may become less predictable in a future warmer climate due to the weakened circulation. We also physically explain our results by relating weaker circulations to the increase in the vertical dry static energy gradient in a warmer climate.

1. Introduction

The Madden-Julian Oscillation (MJO) is the dominant mode of tropical intraseasonal variability (Madden & Julian, 1971, 1972; Zhang, 2005, 2013). Understanding how MJO activity may change in a future warmer climate is important because of the profound impacts that the MJO has on various parts of the globe. MJO activity can modulate the mean climate state (Sardeshmukh & Sura, 2007), the onset and break of monsoon systems (Lau & Waliser, 2012), the formation of tropical storms (e.g., Maloney & Hartmann, 2000), the initiation of El Niño events (e.g., Hendon et al., 2007), tropical-extratropical interactions and extreme events in the extratropics (Baggett et al., 2017; Cassou, 2008; Henderson et al., 2017; Mundhenk et al., 2018), and the deep ocean (Matthews et al., 2007). Many of these effects result from wind variability associated with the MJO, and hence the ability to produce and predict the MJO-induced modulation of these various phenomena depends upon the ability of the MJO to produce robust wind variability (e.g., Mundhenk et al., 2018).

Global warming-induced variations in the MJO have been studied in both historical climate records (Jones & Carvalho, 2006; Slingo et al., 1999) and numerical simulations ranging from idealized aquaplanet models (e.g., Maloney et al., 2010) to fully coupled global climate models (GCMs; Adames et al., 2017a; Arnold et al., 2015;

Subramanian et al., 2014). Most (but not all) previous studies have reported an increase in the MJO precipitation variability in a warmer climate (Adames et al., 2017a; Arnold et al., 2015; Carlson & Caballero, 2016; Schubert et al., 2013; Subramanian et al., 2014). Under global warming, increased lower-tropospheric water vapor due to increased surface temperature results in an increase of MJO precipitation amplitude of more than 9.5%/K (Arnold et al., 2015). These precipitation increases are consistent with decreases in gross moist stability of the tropical atmosphere or related quantities (Adames et al., 2017b; Arnold et al., 2015; Wolding et al., 2017). However, changes in MJO wind variability do not necessarily change in the same way (Adames et al., 2017a; Wolding et al., 2017). For example, Maloney and Xie (2013) studied changes in MJO activity in an aquaplanet model for different sea surface temperature (SST) warming patterns. They found that MJO precipitation changes in future climate are highly sensitive to the pattern of SST warming and MJO wind variance changes can be predicted based on the precipitation variance changes if static stability increases are considered and a weak temperature gradient scaling is used (e.g., Sobel & Bretherton, 2000). The analysis of Maloney and Xie (2013) assumed a first baroclinic mode structure to the MJO that is also assumed in this manuscript. More recently, Wolding et al. (2017) documented an increase of MJO precipitation variability and a decrease of MJO wind variability when analyzing control versus $4xCO_2$ simulations of the superparameterized Community Earth System Model. A similar result was found in the Goddard Institute for Space Studies model (Adames et al., 2017a). Chang et al. (2015) analyzed historical and Representative Concentration Pathway 8.5 (RCP8.5) simulations of the ECHAM5-SIT model and showed that the amplitude of MJO precipitation variability increases by about 17% in the future while zonal wind variability changes insignificantly. The studies above were conducted with a limited set of models, and there has not yet been a detailed mechanistic study using a multimodel data set to investigate the covariability in global warming-induced MJO precipitation and wind variance changes.

The differing changes in MJO precipitation and wind variance suggested by the previous studies have parallels to those associated with the mean tropical climate, as tropical static stability changes mediate time mean dry static energy (DSE) transports into or out of the convective regions (Su & Neelin, 2003). In particular, Knutson and Manabe (1995) show using a coupled ocean-atmosphere model in response to quadrupling of CO_2 that time-mean vertical motion in tropical convective regions is reduced slightly even though precipitation amplitude is increased by 15% due to the increase of static stability. Similar arguments on the weakening of the tropical convective mass flux were derived by Held and Soden (2006) and Vecchi and Soden (2007) that reconciled boundary layer moisture increases and more modest precipitation increases in response to changes in the global mean surface radiation budget under global warming conditions.

Previous studies largely analyzed simplified models, a single GCM, or imperfect analogues to global warming in the observational record to examine the influence of global warming on the MJO (e.g., see the discussion in Maloney & Xie, 2013). In this paper, we will examine how MJO precipitation and wind variability change at the end of the 21st century in RCP8.5 using the multimodel data set from Coupled Model Intercomparison Project phase 5 (CMIP5, Taylor et al., 2012). In particular, CMIP5 allows us to re-examine with a broader set of models the hypothesis that MJO precipitation and circulation variance changes in future climate are mediated by changes in tropical static stability as predicted by weak temperature gradient theory (e.g., Maloney & Xie, 2013; Wolding et al., 2017). We will indeed show below that changes in the vertical DSE gradient in a warmer climate are a first order contribution to the relative change in strength of MJO precipitation and wind anomalies in a future warmer climate.

2. Data and Methodology

To examine changes in MJO band precipitation and wind variance, 21st century simulations from the World Climate Research Programme's CMIP5 (Taylor et al., 2012) multimodel data set for RCP8.5 are used. Based on the study of Henderson et al. (2017), only six models with high MJO simulation skill are used (Table 1). Daily mean fields during the historical forcing period of 1986 to 2005 are used to assess MJO activity in current climate and are compared to the time period 2081 to 2100 from RCP8.5. The change in midtroposphere DSE gradient is used to interpret the relative change in MJO precipitation and wind variance. To calculate this change, we use monthly mean fields in place of daily ones for higher vertical resolution (Figures 3 and 4). We only focus on oceanic regions of the tropics in this study to avoid complications of interpretation

Table 1
A List of the Six Models With Relatively Good MJO Performance From CMIP5 Used in This Study

Model	Description	Resolution
BCC-CSM1-1	Beijing Climate Center, China	2.8° × 2.8°
CNRM-CM5	Centre National de Recherches Météorologiques, France	1.4° × 1.4°
GFDL-CM3	NOAA/Geophysical Fluid Dynamics Laboratory	2.0° × 2.5°
MIROC5	Atmosphere and Ocean Research Institute, National Institute for Environmental Studies, and JAMSTEC, Japan	1.4° × 1.4°
MRI-CGCM3	Meteorological Research Institute, Japan	1.1° × 1.1°
NorESM1-M	Norwegian Climate Centre, Norway	1.9° × 2.5°

caused by topography in calculating static stability and how it modulates the diabatic heating-wind relationship through weak temperature gradient theory.

All data except for those used in the static stability climatology were first band-pass filtered to 30–90 days to retain timescales characteristic of the MJO band. Boreal winter (November to April) intraseasonal variability is defined by analyzing the variance and standard deviation of band-pass filtered data. Global warming-induced changes of all variables used in the analysis are normalized by the corresponding climatological mean (average of historical and global warming simulations) before taking the domain average.

3. Results

3.1. Basic Assessment of Wind and Precipitation Variability Changes

Figures 1a, 1c, and 1e show the multimodel mean MJO band precipitation, 850-hPa zonal wind, and 500 hPa omega variance over the tropical oceans during boreal winter in the historical simulations. Large MJO precipitation variance is found in the western Pacific and Indian Oceans, resembling the observed variance distribution as well as the climatological mean precipitation pattern (see Waliser et al., 2009 and Figure S1a in the supporting information). Under global warming, multimodel mean MJO precipitation variance increases in most areas of the tropics relative to the control, consistent with previous individual modeling studies (e.g., Wolding et al., 2017). Increases are found not only in the western Pacific and Indian Oceans (Figure 1b) but also in the central and east Pacific, consistent with the mean SST changes and the decrease of gross moist stability in the tropical regions (see Benedict et al., 2014; Maloney & Xie, 2013; Xie et al., 2010). In isolation, existing MJO convective regions would be expected to increase in precipitation variance through increased

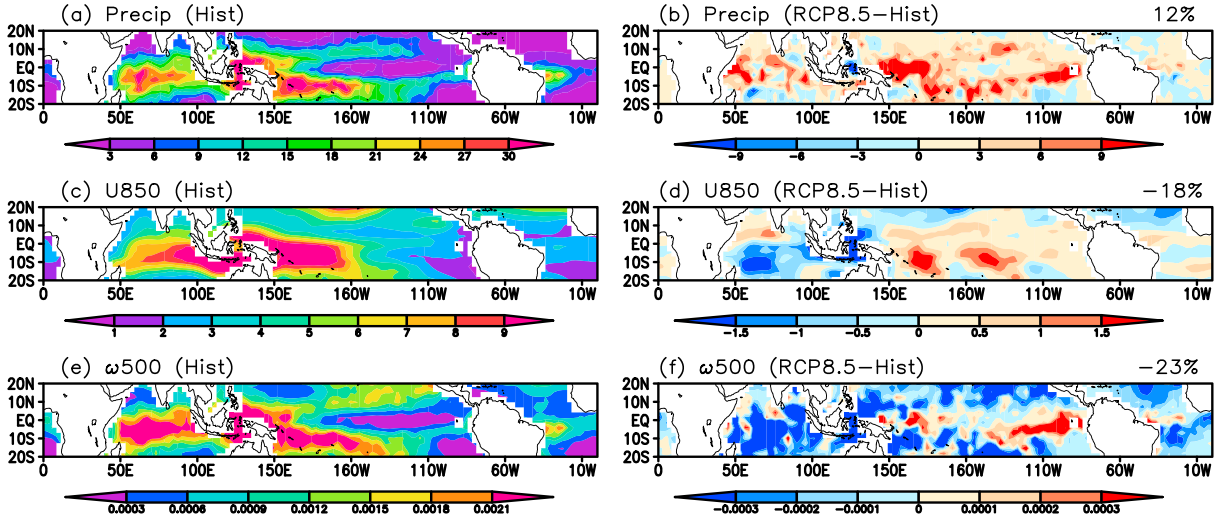

Figure 1. Spatial distribution of variance of 30–90 day filtered (a and b) precipitation ($mm^2\ day^{-2}$), (c and d) 850 hPa zonal wind ($m^2\ s^{-2}$), and (e and f) 500 hPa omega ($Pa^2\ s^{-2}$) for the historical simulation and difference between RCP8.5 and historical simulations, respectively. The value on the top-right corner of (b), (d), and (f) shows the percentage changes averaged over the domain of 10°S-0, 90°E-180. We note that the precipitation, 850 hPa zonal wind and 500 hPa omega variance change patterns shown here are dominated by two models (BCC-CSM1-1 and MRI-CGCM3), as indicated in Figures S2–S4.

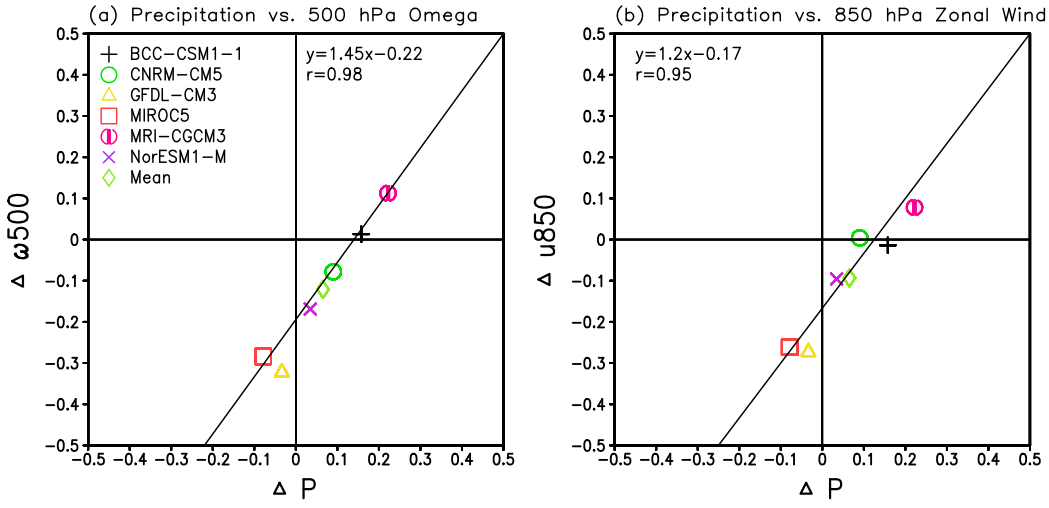

Figure 2. Differences in the 30- to 90-day standard deviation of precipitation (*x*-axis) and (a) 500 hPa omega and (b) 850 hPa zonal wind in RCP8.5 relative to the historical simulation. All the values have been normalized by the average between the historical and RCP8.5 simulations.

lower tropospheric moisture and decreased gross moist stability (e.g., Arnold et al., 2013; Chou et al., 2009), although quantifying this behavior in the CMIP5 simulations we analyze is a topic of future work.

To compare the relative change in multimodel mean MJO-band precipitation to corresponding atmospheric circulation changes, we first show the historical simulation pattern of the 850 hPa zonal wind and 500 hPa omega variance (Figures 1c and 1e). As shown, their pattern distributions are broadly similar to that of MJO precipitation variance, and also the distribution of wind variance in observations (Waliser et al., 2009). However, under global warming, despite the increase in MJO precipitation variance, both the multimodel mean zonal wind and omega variance show decreases over the Indo-Pacific warm pool, consistent with individual model studies (e.g., Maloney & Xie, 2013; Wolding et al., 2017), and may be related to increases in static stability in a warmer climate. MJO wind variance increases over the central and east Pacific, likely associated with the further eastward extent of MJO activity in a warmer climate associated with El Niño-like SST warming there.

Now we examine the changes in MJO precipitation and wind/omega variability for each model averaged over the southern warm pool region (10°S-0, 90°E-180), where MJO wind and precipitation variance maximizes during boreal winter (Figure 1). Results shown below are not sensitive to the exact bounds used for this regional average. In Figure 2a, four of six models show increases in the standard deviation of 30- to 90-day precipitation in a warmer climate relative to today. Changes range from a 10% decrease in precipitation amplitude to about a 20% increase. While the multimodel mean increase in MJO precipitation amplitude is about 7%, MJO precipitation amplitude can decrease in a future warmer climate in some models, contrary to expectations of previous studies with single GCMs. We note however that Maloney and Xie (2013) showed that precipitation variance changes in future climate are sensitive to the warming pattern, a result that could explain some of this discrepancy, although we leave investigation of the sensitivity to warming pattern to future work. The change in 500 hPa omega amplitude is also shown in Figure 2a, indicating a sign of change not necessarily consistent with that of precipitation change. Four of six models show decreases in omega variability at 500 hPa, for a multimodel decrease in amplitude of about 10%. Interestingly, changes in omega amplitude relative to precipitation fall along a straight line with a slope near one, offset from the origin. If the relationship between MJO wind and precipitation variability is regulated by weak temperature gradient theory as suggested by Maloney and Xie (2013), omega and precipitation variability should be related in the following way using the dominant thermodynamic balance (Sobel & Bretherton, 2000):

$$Q' \approx \omega' \frac{\partial \overline{s}}{\partial p} \tag{1}$$

where Q is apparent heat source that in the vertical integral is approximately proportional to precipitation in convective regions, ω is vertical velocity, and $\frac{\partial s}{\partial p}$ is the vertical DSE gradient ($s = c_p T + gz$, with T is temperature, g is gravity, z is the height, and c_p is specific heat of dry air at constant pressure). The primes term $()'$ denote the standard deviation of the fields on the MJO timescales, while the bar $\overline{()}$ denotes the climatological mean. Changes among the terms in (1) from future to current climate (Δ) can be related in the following way (taking advantage of the proportionality of Q' and precipitation anomalies P' in convective regions; Maloney & Xie, 2013):

$$\frac{\Delta\omega'}{\omega'} = \frac{\Delta P'}{P'} - \frac{\Delta\left(\frac{\partial \bar{s}}{\partial p}\right)}{\frac{\partial \bar{s}}{\partial p}} \tag{2}$$

For a line of slope 1 and identical static stability change across models, the fractional change in static stability near 500 hPa would represent the *x*-intercept or opposite of the *y*-intercept in Figure 2a. This would suggest a fractional static stability increase about 20% by the end of the 21st century, which is indeed what we calculate below in Figure 4. However, the slope of the line in Figure 2 does differ a bit from one with modestly different *x*-intercept and *y*-intercept, likely reflecting the difference in static stability changes (and climate sensitivities) among models.

The 850 hPa zonal wind standard deviation changes shows a generally consistent result to that of 500 hPa omega (Figure 2b), as would be expected through mass continuity under the assumption of a first baroclinic mode (Maloney & Xie, 2013). We assume for this scale analysis that the MJO spatial scale remains invariant under global warming. However, any MJO spatial scale changes would also be expected to affect the relationship between 500 and 850 hPa horizontal wind changes and may contribute to the different least squares fit slopes produced in Figures 2a and 2b (Á. Adames, personal communication, May 31, 2018). However, we leave further exploration of the impact of spatial scale changes to future work. In summary, under the global warming scenario, the multimodel mean MJO precipitation amplitude tends to increase while MJO circulation amplitude decreases, consistent with previous studies (Arnold et al., 2015; Maloney & Xie, 2013; Wolding et al., 2017), although these results do not generalize to individual models. The precipitation variance changes appear to consistently scale with wind variance changes from model to model as mediated by changes in tropical static stability.

We note that in addition to the analysis of broader intraseasonal variance shown above, we assessed variance changes in a narrower MJO band centered on eastward zonal wave numbers 1–3 and frequencies of 30–90 days. After averaging fields between 0°S and 10°S, doing a decomposition in wave number-frequency space for boreal winter, and then integrating variance in the MJO wave number and frequency bands, the multimodel mean MJO precipitation amplitude increases by 20.9% in the RCP8.5 simulation relative to the control, whereas the 850 hPa wind variance decreases by 1.1%. This result is consistent with the analysis of broader variance discussed above, and holds despite increases in wind variance in the east Pacific in Figure 1d.

3.2. Predicting the Changes in Ratio of Precipitation to Wind Amplitude Based on Static Stability

We noted that the relationship between MJO wind amplitude changes and precipitation amplitude changes in Figure 2 is offset from the origin, implying different rate of change between precipitation and wind amplitude. We show here that the discrepancy between MJO precipitation and wind amplitude changes under global warming can be explained by static stability changes.

The vertical structure of DSE change between the end of the 21st century and the historical period averaged over the entire tropics from 20°S to 20°N is shown in Figure 3. Given the weak temperature gradient conditions of the tropics, the vertical profile of DSE change is similar on a regional level. As expected, DSE increases are greater in the upper troposphere versus the lower troposphere, consistent with moist adiabatic adjustment setting the vertical thermal structure of the atmosphere (e.g., Knutson & Manabe, 1995). The vertical DSE gradient is increased in the middle to upper troposphere between 400 and 600 hPa, consistent with the level of maximum convective mass flux in models. As noted above, a more stable atmosphere will result in weakening of the tropical mean atmospheric circulation although tropical precipitation increases (e.g., Held & Soden, 2006; Vecchi & Soden, 2007). We show below that static stability changes are also responsible for MJO wind variance reductions in future climate relative to precipitation variance changes.

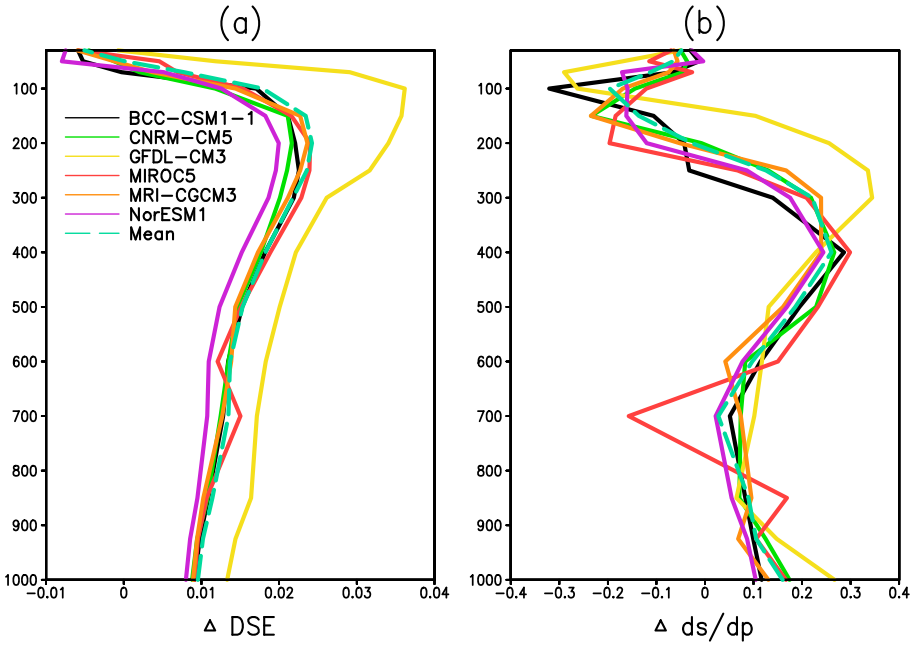

Figure 3. Changes in vertical structure of (a) dry static energy (DSE) and (b) DSE gradient (ds/dp) relative to the historical simulation over the tropical ocean (20°S–20°N). All the values have been normalized by the average of historical and RCP8.5 simulations.

Here we attempt to predict differences in the changes of ratio of MJO precipitation and wind anomalies under global warming based on the changes of static stability. Using the dominant thermodynamic energy balance (1), fractional changes in the ratio of *P* anomalies to omega anomalies in the middle troposphere should scale with static stability changes:

$$\frac{\Delta\left(\frac{P'}{\omega'}\right)}{\left(\frac{P'}{\omega'}\right)} = \frac{\Delta\left(\frac{\partial\bar{s}}{\partial p}\right)}{\left(\frac{\partial\bar{s}}{\partial p}\right)} \tag{3}$$

Again, we represent precipitation, omega, and wind anomalies using the standard deviation of 30- to 90-day band-pass filtered fields. Climatological static stability is averaged in the layer between 400 and 600 hPa

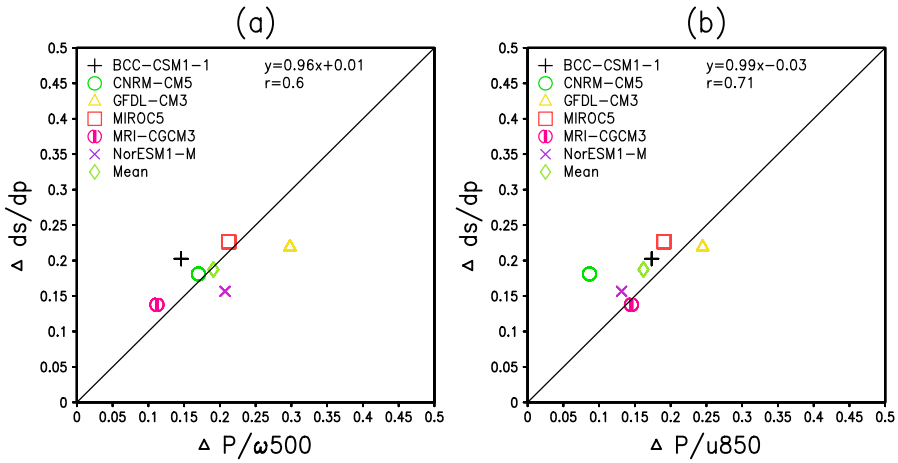

Figure 4. RCP8.5 fractional differences relative to the historical simulation in the dry static energy (DSE) gradient averaged from 400 to 600 hPa (*y*-axis) and the ratio of the standard deviations of 30–90 day precipitations anomalies and a 500 hPa omega anomalies and b 850 hPa zonal wind anomalies (*x*-axis). All the values have been normalized by the average between historical and RCP8.5 simulations.

(average of the RCP8.5 and historical simulations). Figure 4 shows the fractional change in static stability versus the fractional change in the ratio of precipitation standard deviation anomalies to 500 hPa omega standard deviation anomalies (Figure 4a) and 850 hPa zonal wind standard deviation anomalies (Figure 4b). The $\frac{\partial \bar{s}}{\partial p}$ increase varies from about 12% to 30% in RCP8.5 relative to historical, with a multimodel mean increase of about 20%, consistent with the discussion of Figure 2. The multimodel mean change in the ratio of precipitation to omega anomalies is reasonably well predicted by static stability changes. If the theory is correct, there should be a one-to-one relationship between fractional changes in static stability and the ratio of precipitation to omega standard deviation anomalies among models. This is generally true to first order with models in Figure 4a clustering around the line of slope 1, although there is some scatter in this relationship suggesting that other factors exercise influence on this ratio. Similar changes in the ratio between precipitation and 850 hPa zonal wind anomalies and the DSE gradient change are also found (Figure 4b). In general, the relative change of precipitation and wind MJO variance in warmer climate is shown to be sensitive to the vertical structure of temperature and static stability changes, consistent with the results of Maloney and Xie (2013) and Wolding et al. (2017).

4. Concluding Remarks

Predicting precipitation and circulation changes in a future climate is a challenging task owing to the difficulty that general circulation models have at simulating interactions between convection and the large-scale circulation, for example, the simulation of MJO. Here we use six CMIP5 models with high MJO simulation skill (Henderson et al., 2017) to study how MJO precipitation and wind variability is projected to change at the end of the 21st century relative to today under RCP8.5. Compared to previous studies that have used simplified models or individual GCM to study MJO changes in a warmer climate, our current study is the first to assess precipitation and wind variances changes under global warming and assess physical reasons for the different changes in wind versus precipitation variability in a multimodel data set. Our main results are summarized as follow:

1. Under global warming in RCP8.5, the CMIP5 multimodel mean shows a 7% increase in MJO-band precipitation variance and a 10% decrease in its corresponding wind variance (Figures 1 and 2). This is consistent with some previous results from individual models (e.g., Adames et al., 2017a; Wolding et al., 2017)
2. Substantial differences in MJO wind and precipitation variance changes occur among models in response to warming, although most exhibit an increase in MJO precipitation variance with a decrease in MJO wind variance. Even if not negative, MJO wind variance changes are always less than the MJO precipitation variance change (Figure 2).
3. The differences in amplitudes of MJO precipitation and wind amplitude changes for both the multimodel mean and for individual models can be explained/predicted based on the change of the tropical vertical DSE gradient under global warming, consistent with the weak temperature gradient theory (Figure 4).

These results suggest that the impact of MJO on many weather and climate phenomena in a future climate may weaken due to weaker large-scale circulations, including the ability to predict such phenomena. While the current study focuses on the MJO, the results imply a similar weakening of wind anomalies relative to precipitation anomalies during ENSO events in a warming climate. Future work will examine whether MJO teleconnections to higher latitudes weaken in the majority of CMIP5 models in response to climate warming, including effects on extreme events such as atmospheric rivers (e.g., Baggett et al., 2017). MJO teleconnections to other parts of the tropics such as the east Pacific and Atlantic where the MJO modulates tropical cyclone activity may also change in strength (e.g., Maloney & Hartmann, 2000). There may be conflicting effects from MJO variance shifting eastward in a warmer climate toward the east Pacific and Atlantic (e.g., Figure 1) versus MJO wind circulations decrease in strength. We are also interested in explaining the differences in MJO precipitation amplitude change from model to model associated with the changes in vertical structure of convection, for example, deep and shallow convection. Such studies are currently being done and will be published in forthcoming papers.

Acknowledgments
We thank Ángel Adames and one anonymous reviewer for insightful comments that helped improve the manuscript. We also thank Haibo Liu and the Lamont-Doherty Earth Observatory for obtaining the CMIP5 data and the World Climate Research Programme's Working Group on Coupled Modeling, which is responsible for CMIP. The CMIP5 data sets used in this article were downloaded from the Earth System Grid Federation at Lawrence Livermore National Laboratory, Department of Energy, USA at https://pcmdi9.llnl.gov/projects/cmip5/. This work was supported by the National Science Foundation under grant AGS-1441916, and the NOAA MAPP program under grants NA15OAR4310098 and NA15OAR4310099. The statements, findings, conclusions, and recommendations do not necessarily reflect the views of NOAA or NSF.

References

Adames, Á. F., Kim, D., Sobel, A. H., Del Genio, A., & Wu, J. (2017a). Changes in the structure and propagation of the MJO with increasing CO_2. *Journal of Advances in Modeling Earth Systems*, *9*(2), 1251–1268. https://doi.org/10.1002/2017MS000913

Adames, Á. F., Kim, D., Sobel, A. H., Del Genio, A., & Wu, J. (2017b). Characterization of moist processes associated with changes in the propagation of the MJO with increasing CO_2. *Journal of Advances in Modeling Earth Systems*, *9*, 2946–2967. https://doi.org/10.1002/2017MS001040

Arnold, N., Kuang, Z., & Tziperman, E. (2013). Enhanced MJO-like variability at high SST. *Journal of Climate*, *26*(3), 988–1001. https://doi.org/10.1175/JCLI-D-12-00272.1

Arnold, N. P., Branson, M., Kuang, Z., Randall, D. A., & Tziperman, E. (2015). MJO intensification with warming in the superparameterized CESM. *Journal of Climate*, *28*(7), 2706–2724. https://doi.org/10.1175/JCLI-D-14-00494.1

Baggett, C. F., Barnes, E. A., Maloney, E. D., & Mundhenk, B. D. (2017). Advancing atmospheric river forecasts into subseasonal timescales. *Geophysical Research Letters*, *44*, 7528–7536. https://doi.org/10.1002/2017GL074434

Benedict, J. J., Maloney, E. D., Sobel, A. H., & Frierson, D. M. (2014). Gross moist stability and MJO simulation skill in three full-physics GCMs. *Journal of the Atmospheric Sciences*, *71*(9), 3327–3349. https://doi.org/10.1175/JAS-D-13-0240.1

Carlson, H., & Caballero, R. (2016). Enhanced MJO and transition to superrotation in warm climates. *Journal of Advances in Modeling Earth Systems*, *8*(1), 304–318. https://doi.org/10.1002/2015MS000615

Cassou, C. (2008). Intraseasonal interaction between the Madden-Julian oscillation and the North Atlantic oscillation. *Nature*, *455*(7212), 523–527. https://doi.org/10.1038/nature07286

Chang, C.-W. J., Tseng, W.-L., Hsu, H.-H., Keenlyside, N., & Tsuang, B.-J. (2015). The Madden-Julian oscillation in a warmer world. *Geophysical Research Letters*, *42*, 6034–6042. https://doi.org/10.1002/2015GL065095

Chou, C., Neelin, J. D., Chen, C.-A., & Tu, J.-Y. (2009). Evaluating the "Rich-Get-Richer" mechanism in tropical precipitation change under global warming. *Journal of Climate*, *22*(8), 1982–2005. https://doi.org/10.1175/2008JCLI2471.1

Held, I. M., & Soden, B. J. (2006). Robust responses of the hydrological cycle to global warming. *Journal of Climate*, *19*(21), 5686–5699. https://doi.org/10.1175/JCLI3990.1

Henderson, S. A., Maloney, E. D., & Son, S.-W. (2017). Madden–Julian oscillation Pacific teleconnections: The impact of the basic state and MJO representation in general circulation models. *Journal of Climate*, *30*(12), 4567–4587. https://doi.org/10.1175/JCLI-D-16-0789.1

Hendon, H. H., Wheeler, M. C., & Zhang, C. (2007). Seasonal dependence of the MJO–ENSO relationship. *Journal of Climate*, *20*(3), 531–543. https://doi.org/10.1175/JCLI4003.1

Jones, C., & Carvalho, L. M. V. (2006). Changes in the activity of the Madden–Julian oscillation during 1958–2004. *Journal of Climate*, *19*(24), 6353–6370. https://doi.org/10.1175/JCLI3972.1

Knutson, T. R., & Manabe, S. (1995). Time-mean response over the tropical Pacific to increased CO_2 in a coupled ocean–atmosphere model. *Journal of Climate*, *8*(9), 2181–2199. https://doi.org/10.1175/1520-0442(1995)008<2181:TMROTT>2.0.CO;2

Lau, W. K.-M., & Waliser, D. E. (2012). *Intraseasonal variability in the atmosphere-ocean climate system*. Berlin, Heidelberg: Springer. https://doi.org/10.1007/978-3-642-13914-7

Madden, R. A., & Julian, P. R. (1971). Detection of a 40–50 day oscillation in the zonal wind in the tropical Pacific. *Journal of the Atmospheric Sciences*, *28*(5), 702–708. https://doi.org/10.1175/1520-0469(1971)028<0702:DOADOI>2.0.CO;2

Madden, R. A., & Julian, P. R. (1972). Description of global-scale circulation cells in the Tropics with a 40–50 day period. *Journal of the Atmospheric Sciences*, *29*(6), 1109–1123. https://doi.org/10.1175/1520-0469(1972)029<1109:DOGSCC>2.0.CO;2

Maloney, E. D., & Hartmann, D. L. (2000). Modulation of hurricane activity in the Gulf of Mexico by the Madden-Julian oscillation. *Science*, *287*(5460), 2002–2004. https://doi.org/10.1126/science.287.5460.2002

Maloney, E. D., Sobel, A. H., & Hannah, W. M. (2010). Intraseasonal variability in an aquaplanet general circulation model. *Journal of Advances in Modeling Earth Systems*, *2*, 5. https://doi.org/10.3894/JAMES.2010.2.5

Maloney, E. D., & Xie, S.-P. (2013). Sensitivity of tropical intraseasonal variability to the pattern of climate warming. *Journal of Advances in Modeling Earth Systems*, *5*(1), 32–47. https://doi.org/10.1029/2012MS000171

Matthews, A. J., Singhruck, P., & Heywood, K. J. (2007). Deep ocean impact of a Madden-Julian oscillation observed by Argo floats. *Science*, *318*(5857), 1765–1769. https://doi.org/10.1126/science.1147312

Mundhenk, B. D., Barnes, E. A., Maloney, E. D., & Baggett, C. F. (2018). Skillful subseasonal prediction of atmospheric river activity based on the Madden-Julian oscillation and the Quasi-Biennial oscillation. *Nature (npj) Climate Atmospheric Science*, *1*(1), 1. https://doi.org/10.1038/s41612-017-0008-2

Sardeshmukh, P. D., & Sura, P. (2007). Multiscale impacts of variable heating in climate. *Journal of Climate*, *20*(23), 5677–5695. https://doi.org/10.1175/2007JCLI1411.1

Schubert, J. J., Stevens, B., & Crueger, T. (2013). Madden-Julian Oscillation as simulated by the MPI earth system model: Over the last and into the next Millennium. *Journal of Advances in Modeling Earth Systems*, *5*, 71–84. https://doi.org/10.1029/2012MS000180

Slingo, J. M., Rowell, D. P., Sperber, K. R., & Nortley, F. (1999). On the predictability of the interannual behaviour of the Madden-Julian oscillation and its relationship with El Niño. *Quarterly Journal of the Royal Meteorological Society*, *125*(554), 583–609. https://doi.org/10.1002/qj.49712555411

Sobel, A. H., & Bretherton, C. S. (2000). Modeling tropical precipitation in a single column. *Journal of Climate*, *13*(24), 4378–4392. https://doi.org/10.1175/1520-0442(2000)013<4378:MTPIAS>2.0.CO;2

Su, H., & Neelin, J. D. (2003). The scatter in tropical average precipitation anomalies. *Journal of Climate*, *16*(23), 3966–3977. https://doi.org/10.1175/1520-0442(2003)016<3966:TSITAP>2.0.CO;2

Subramanian, A., Jochum, M., Miller, A. J., Neale, R., Seo, H., Waliser, D., & Murtugudde, R. (2014). The MJO and global warming: A study in CCSM4. *Climate Dynamics*, *42*(7-8), 2019–2031. https://doi.org/10.1007/s00382-013-1846-1

Taylor, K. E., Stouffer, R. J., & Meehl, G. A. (2012). An overview of CMIP5 and the experiment design. *Bulletin of the American Meteorological Society*, *93*(4), 485–498. https://doi.org/10.1175/BAMS-D-11-00094.1

Vecchi, G. A., & Soden, B. J. (2007). Global warming and the weakening of the tropical circulation. *Journal of Climate*, *20*(17), 4316–4340. https://doi.org/10.1175/JCLI4258.1

Waliser, D. E., Sperber, K., Hendon, H., Kim, D., Maloney, E., & Wheeler, M. (2009). MJO simulation diagnostics. *Journal of Climate*, *22*(11), 3006–3030. https://doi.org/10.1175/2008JCLI2731.1

Wolding, B. O., Maloney, E. D., Henderson, S., & Branson, M. (2017). Climate change and the Madden-Julian oscillation: A vertically resolved weak temperature gradient analysis. *Journal of Advances in Modeling Earth Systems*, *9*(1), 307–331. https://doi.org/10.1002/2016MS000843

Xie, S.-P., Deser, C., Vecchi, G. A., Ma, J., Teng, H., & Wittenberg, A. T. (2010). Global warming pattern formation: Sea surface temperature and rainfall. *Journal of Climate*, *23*(4), 966–986. https://doi.org/10.1175/2009JCLI3329.1

Zhang, C. (2005). Madden-Julian oscillation. *Reviews of Geophysics*, *43*, RG2003. https://doi.org/10.1029/2004RG000158

Zhang, C. (2013). Madden–Julian oscillation: Bridging weather and climate. *Bulletin of the American Meteorological Society*, *94*(12), 1849–1870. https://doi.org/10.1175/BAMS-D-12-00026.1